

Nonlinear dynamics of resonant stimulated Cerenkov emission in a spatially bounded plasma

M. A. Krasil'nikov, M. V. Kuzelev, and A. A. Rukhadze

Institute of General Physics, Russian Academy of Sciences, 117942 Moscow, Russia

(Submitted 20 March 1995)

Zh. Éksp. Teor. Fiz. **108**, 521–530 (August 1995)

We discuss the nonlinear nonstationary problem of resonant Cerenkov radiation by a magnetized relativistic high-current electron beam with a front propagating in a transverse-uniform plasma waveguide of finite length. Using numerical simulation we demonstrate the existence of optimal values for the beam-plasma system parameters corresponding to maximum amplitude of the wave radiated at the output. When the optimal beam current is chosen, an almost steady value of the amplitude of the output radiation is observed. Further increases in the current destroy the steady state: the output radiation becomes chaotic, and the radiated power stops increasing. © 1995 American Institute of Physics.

1. Interest in the study of stimulated emission, or, equivalently, beam-plasma instabilities in systems of finite length, is not only theoretical. The range of practical applications that involve these instabilities is extensive, a fact that motivates experimentalists to study them intensely even today. Among these applications we should list transport of high-power beams through a neutral plasma background,¹ excitation of comparatively slow waves in a plasma in order to accelerate ions,² etc. Our interest is in using these beam instabilities to excite coherent electromagnetic oscillations in a plasma and radiate them from the plasma, i.e., the problem of a plasma oscillator.³ The task of this paper is to investigate the theoretical aspects of this problem.

It is well known that a radiative resonant Cerenkov instability develops in the electrodynamic structure of a plasma oscillator.⁴ In this case, waves are excited in the plasma with phase velocities close to the velocity of the electron beam. Experiments^{2,5,6} and numerical calculations based on direct solution of the full system of Maxwell-Vlasov equations⁷ show that the average frequency ω of radiation from the plasma is considerably larger than the width of the radiation spectrum $\delta\omega$:

$$\delta\omega \ll \omega. \quad (1)$$

The frequency itself is close to the frequency of exact Cerenkov resonance:

$$\omega = \sqrt{\omega_p^2 - k_{\perp}^2 u^2 \gamma^2}, \quad (2)$$

where ω_p is the Langmuir plasma frequency, k_{\perp} is the transverse wave number of the electrodynamic structure of the oscillator, u is the beam velocity, and $\gamma = (1 - u^2/c^2)^{-1/2}$.

Condition (1) allows us to develop a fairly simple model (compared to Ref. 7) of the plasma oscillator based on the method of slowly-varying amplitudes^{8–10}. At this point, we should note that both (1) and (2) are violated at high beam currents, which limits the range of applicability of the simplified model we will discuss below.¹⁰ As shown in Refs. 10, 11, a reliable criterion to ensure that (1) and (2) are fulfilled is the condition

$$J_b \leq J_0, \quad (3)$$

where J_b is the beam current and J_0 is the limiting vacuum current.¹² If a metallic waveguide of radius R is used as the electrodynamic structure for the oscillator, and the beam is in the form of a thin tube, then

$$J_0 = \frac{mc^3}{e} \frac{(\gamma^{2/3} - 1)^{3/2}}{\Delta/r_b + 2 \ln(R/r_b)}, \quad (4)$$

where r_b is the beam radius and Δ is its thickness.

We should also note that the beam instability in a plasma waveguide in the linear and nonlinear stages of evolution was discussed rather thoroughly in Refs. 13, 14. However, in the majority of cases, this instability has been treated for beams and waveguides of infinite length, which corresponds to the classical initial-value, boundary-value, and initial-boundary-value problems.¹⁵ Although these problems are important for understanding the physics of the phenomenon and for designing plasma amplifiers,¹⁶ they are insufficient for the study of plasma oscillators. For this reason, there is interest in studying the nonlinear dynamics of systems of finite length where the wave excited by the beam is reflected from the radiating horn.

2. Consider a waveguide in the region $z \geq 0$ with metal walls. Let the segment of waveguide $0 \leq z \leq L$ be filled with a uniform plasma strongly magnetized by an external longitudinal magnetic field. We will treat the boundary $z = L$ between plasma and vacuum as infinitely sharp, which is the simplest model of a radiating horn. At the waveguide boundary $z = 0$ itself, we place a constriction, which ensures that this boundary will not be completely transparent at the operating frequency of the oscillator.

Assume that at time $t = 0$ we begin to inject a fully magnetized electron beam with a sharp front into the waveguide through the boundary $z = 0$.¹ We will not include the processes of charge neutralization, reverse current generation, etc.,¹⁷ which are unimportant here; rather, we will limit ourselves to discussing the interaction of the beam with the microwave fields alone. Due to spontaneous Cerenkov radiation, the injected electron beam excites a copropagating wave of frequency ω (Ref. 2). As it propagates into the re-

gion $z \geq 0$, this wave is partially reflected from the radiating horn at $z=L$. For the usual model of a horn, the reflection coefficient has the form:¹⁰

$$\kappa = \frac{n(\omega_p) - n(0)}{n(\omega_p) + n(0)}, \quad (5)$$

where $n^2(\omega_p) = 1 - k_{\perp}^2 c^2 / (\omega^2 - \omega_p^2)$. The reflected counter-propagating wave has the same frequency ω , but propagates in the direction opposite to the copropagating wave. Due to the beyond-cutoff constriction at $z=0$, the counterpropagating wave is entirely converted at this point into a copropagating wave.

We present here a brief derivation of the equations that describe the interaction of the beam, the copropagating wave, and the counterpropagating wave. We should note immediately that the counterpropagating wave, which is not in Cerenkov resonance with the beam, does not interact with it on the average; it arises only from reflection from the boundary $z=L$. Once it is reflected at $z=0$, the counterpropagating wave creates a copropagating wave, which interacts with the beam and is amplified by stimulated Cerenkov emission. Furthermore, as shown in Ref. 18, the electrons of the plasma may be treated in the linear approximation.

Let us begin with the wave equation for the polarization potential of a TM waveguide mode¹⁹

$$\frac{\partial}{\partial z} \left(\Delta - \frac{1}{c^2} \frac{\partial^2}{\partial t^2} \right) \Psi = 4\pi(\rho_p + \rho_b). \quad (6)$$

The perturbation of the electron charge density ρ_p of the plasma is determined in the linear approximation by the equations

$$\frac{\partial^2 \rho_p}{\partial t^2} = -\frac{\omega_p^2}{4\pi} \frac{\partial E_z}{\partial z}, \quad E_z = \left(\frac{\partial^2}{\partial z^2} - \frac{1}{c^2} \frac{\partial^2}{\partial t^2} \right) \Psi, \quad (7)$$

where E_z is the longitudinal component of the electric field. As for the beam charge density perturbation ρ_b , it is convenient to calculate it by using the expression²⁰

$$\rho_b = e \delta(r_{\perp} - r_b) \sum \delta(z - z_j) \left(\frac{n_b S_b \lambda}{N} \right). \quad (8)$$

Here r_{\perp} is the coordinate in the transverse cross section of the waveguide, r_b is the transverse position of the thin beam, z_j is the longitudinal position of the j th electron, n_b is the electron beam density, S_b is the area of the transverse beam cross section, and λ is a certain characteristic length in the longitudinal direction (see below). It is obvious that N is the number of electrons (macroparticles) in a segment of unperturbed beam of length λ . The coordinates z_j are determined from the relativistic equations of motion:

$$\frac{dz_j}{dt} = v_j, \quad \frac{dv_j}{dt} = \frac{e}{m} \left(1 - \frac{v_j^2}{c^2} \right)^{3/2} E_z(z_j, t). \quad (9)$$

Taking (1) and (2) into account, we seek a solution to Eq. (6) in the form

$$\psi = \frac{1}{2} \left[\left(\sum_{n=1}^{\infty} A_n(z, t) \varphi_n(r_{\perp}) \right) e^{-\omega t + i k_z z} + \text{c.c.} \right], \quad (10)$$

where φ_n are membrane eigenfunctions of the waveguide, A_n is a slowly varying function of z and t , and $k_z = \omega/u$, which takes into account the condition for Cerenkov resonance. It is obvious that if we use this definition of k_z , we must set $\lambda = 2\pi/k_z = 2\pi u/\omega$.

The beam interacts resonantly with only one transverse mode in the solution (10); for definiteness we assume this is the m -th mode. In this case, we should understand by k_{\perp} in (2) the quantity $k_{\perp m}$.²⁾ The most interesting case is, of course, $m=1$. The other transverse modes are excited non-resonantly due to the distortion of the transverse structure of the field by the beam.

From here, we can substitute (10) into (6), taking into account the orthogonality of the φ_n , and average with respect to z over a spatial period equal to λ . When we do this, we obtain equations for the amplitudes A_n . The equation for the resonant amplitude A_m cannot be simplified any more. As for the nonresonant amplitudes A_n ($n \neq m$), when (3) is satisfied they can be calculated explicitly.²¹ This latter step allows us to greatly simplify the right side of the second equation (9). Omitting the lengthy calculations whose essence is described above (see also Ref. 10), we present the final result of transforming Eqs. (6)–(9):

$$\frac{u}{v_g} \frac{\partial a_m}{\partial \tau} + \frac{\partial a_m}{\partial x} = \nu G_m \langle \rho \rangle, \quad \frac{dx_j}{d\tau} = \frac{v_j}{u}, \quad (11)$$

$$\begin{aligned} \gamma^{-3} \frac{d}{d\tau} \left[\frac{v_j}{u} \left(1 - \frac{v_j^2}{c^2} \right)^{-1/2} \right] &= -\frac{1}{2} [a_m(x_j, \tau) e^{i(x_j - \tau)} \\ &+ \text{c.c.}] + i \left\{ \left(\gamma^2 \nu G_m G_{\rho m} \langle \rho \rangle - \frac{\omega_p^2}{k_{\perp m}^2 u^2 \gamma^2} \frac{\partial a_m}{\partial \tau} \right) e^{i(x_j - \tau)} \right. \\ &\left. - \text{c.c.} \right\}. \end{aligned}$$

Here

$$v_g = u \frac{\omega_p^2 - \omega^2}{\omega_p^2 - (u^2/c^2)\omega^2} \quad (12)$$

is the group velocity of the plasma wave, and

$$G_m = S_b \frac{\varphi_m^2(r_b)}{\|\varphi_m\|^2} \quad (13)$$

is a geometric beam factor; the complicated expression for the geometric space charge factor $G_{\rho m}$ for the beam can be found, e.g., in Ref. 21. The beam density enters into (11) through the parameter ν , defined by the expression

$$\nu = \frac{1}{2} \frac{\omega_b^2 \gamma^{-7}}{k_{\perp}^2 u^2}. \quad (14)$$

In writing the equations (11) we have used the dimensionless variables

$$\begin{aligned} \tau = \omega t, \quad x = k_z z, \quad x_j = k_z z_j \\ a_m = \frac{e}{m} \frac{k_z}{\gamma^5 u^2} \varphi_m(r_b) A_m, \end{aligned} \quad (15)$$

The expression for $\langle \rho \rangle$, i.e., the function (8) averaged over z and the transverse cross section of the resonance harmonics, is

$$\langle \rho \rangle = \frac{2}{N} \sum_j e^{-i(x_j - \tau)} \theta(x_j - x + \pi) \theta(x + \pi - x_j), \quad (16)$$

where θ is the Heaviside function. We note that the equation similar to (11) obtained in Ref. 10 is an approximation because not all of the terms given here were included.

Let us discuss the counterpropagating wave. We will denote its slowly varying dimensionless amplitude by b_m . Since the counterpropagating wave does not interact with the beam (on the average), and propagates counter to the beam direction, the equation for b_m is obvious:

$$\frac{u}{v_g} \frac{\partial b_m}{\partial \tau} - \frac{\partial b_m}{\partial x} = 0. \quad (17)$$

The only connection between a_m and b_m is via the following reflection conditions at the boundaries $z=0$ and $z=L$:

$$b_m(x = k_z L, \tau) = \kappa a_m(x = k_z L, \tau), \quad (18)$$

$$a_m(x = 0, \tau) = b_m(x = 0, \tau),$$

where the coefficient κ is defined in (5). Equations (11), (16), (17) and (18) constitute a closed problem, which is solved numerically.

3. Let us first consider some results from linear theory.^{22,23} In the presence of feedback, i.e., when $\kappa \neq 0$, holds the frequency ω acquires a complex correction $\delta\omega$ which is quite complicated in form.¹⁰ For $\text{Im}(\delta\omega) > 0$ the field in the structure grows, implying that it is self-excited, i.e., oscillation begins. The equation $\text{Im}(\delta\omega) = 0$ determines the startup condition for the beginning of oscillations.

For low-current beams when $|\kappa| \ll 1$ holds, the expression for $\delta\omega$ simplifies greatly.²²

$$\delta\omega = \frac{i \left[\frac{\sqrt{3}}{2} \xi - \ln(3/|\kappa|) \right] - \frac{1}{2} \xi}{L/W_g + L/v_g}, \quad (19)$$

where $W_g = 3v_g u / (2v_g + u)$ is the drift velocity during the amplification stage, $\xi = k_z L v_0^{1/3}$, and $v_0 = vG_m$.

From (19) we obtain the equation $\text{Im}(\delta\omega) = 0$ in explicit form:

$$\xi = \frac{2}{\sqrt{3}} \ln(3/|\kappa|). \quad (20)$$

For small ξ , the oscillations in the structure decay, while for large ξ the system oscillates. In general, the startup condition can only be evaluated numerically (see Fig. 1). The system is self-excited if ξ lies above the curve shown in Fig. 1. This is fully confirmed by numerical calculations. Calculations with the feedback switched off ($\kappa=0$) imply that an optimum oscillation regime exists in the region above startup, i.e., for certain values of ξ the wave reflected from the radiating horn will cause feedback most efficiently once the latter is switched on. In this case, the value of the amplitude $|a_m|$

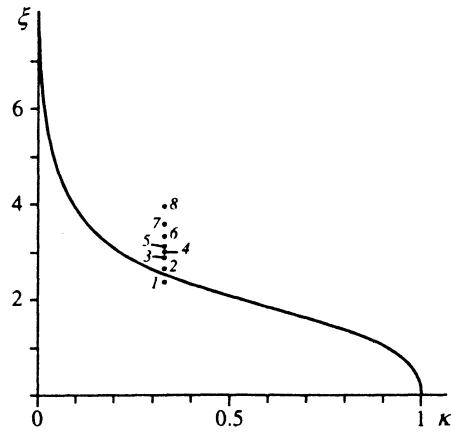


FIG. 1. Startup conditions for oscillations.

established at the output ($z=L$) is close to the maximum value this amplitude can have when the system acts as a pure amplifier (see below).

We note further that, in addition to other corrections, $\delta\omega$ is proportional to $v_g/L \sim \mu/L$. Consequently, in the regime far above startup the field in the structure increases within a time on the order of the propagation time of the beam and electrons over the length of the oscillator (for any method of creating the initial perturbation).

4. We now present the results of our numerical simulation. A structure was designed with parameters close to those of a real experiment:⁶ a cylindrical waveguide with radius $R=1.8$ cm, filled with plasma to a length $L=16$ cm. A thin hollow beam of radius $r_b=0.8$ cm and thickness $\Delta=0.1$ cm excites the fundamental mode of plasma oscillations ($m=1$). The relativistic factor for the beam is $\gamma=2$.

Let us present the results of calculations for $\kappa=0.33$ ($\omega_p = 8 \cdot 10^{10} \text{s}^{-1}$, $\omega = 4.6 \cdot 10^{10} \text{s}^{-1}$). Similar results are also obtained for other reflection coefficients. We varied the parameter ξ , whose values are denoted by the numbered points in Fig. 1. In order to compare with dimensional parameters, we refer to Table I, which lists the ratio of beam current to the maximum vacuum current J_b/J_0 (for the specified parameters, the latter was $J_0=4.52$ kA) and the average radiation efficiency are computed from the expression:

$$\langle \eta \rangle = \left\langle \frac{P_w}{P_b} \right\rangle_\tau, \quad (21)$$

where P_w is the wave power at the output, P_b is the input power of the beam, and the angle brackets imply averaging over time.

Incidentally, it is clear from (19) that $|\delta\omega/\omega| \sim v_0^{1/3}$. From the third column of Table I we see that $v_0^{1/3} \ll 1$ holds, i.e., for the systems we have designed here inequality (1) holds. The same is true for inequality (3).

Figure 2 shows the time dependence of the quantity $\eta(\tau)$. One scale division along the τ axis corresponds to the transit time of the wave over the system length L . For $\xi=2.41$ (curve 1 in Fig. 2, point 1 on Fig. 1, respectively) the startup condition is not satisfied and there is no self-

TABLE I.

No.	ξ	ν_0	J_b , kA	J_b/J_0	$\langle\eta\rangle$
1	2.41	0.00045	0.91	0.20	0
2	2.65	0.0006	1.21	0.27	0.18
3	2.92	0.0007	1.42	0.31	0.19
4	3.00	0.0009	1.82	0.40	0.20
5	3.14	0.001	2.02	0.45	0.20
6	3.38	0.00125	2.53	0.50	0.17
7	3.6	0.0015	3.03	0.67	0.13
8	3.96	0.002	4.04	0.89	0.09

excitation. Therefore, oscillations initially excited by the beam front will gradually decay with time. We note that the startup value of ξ for the chosen κ is 2.55.

For $\xi=2.65$ and $\xi=2.79$, the startup condition is fulfilled and self-excitation of the structure is observed (curves 2 and 3 in Fig. 2, points 2 and 3 on Fig. 1). The gradual growth of the output amplitude is clear. However, this regime is still only slightly above startup. Therefore, the radiation efficiency listed in Table I is reached only after a long period of time.

Point 4 on Fig. 1 ($\xi=3.03$) corresponds to curve 4 shown in Fig. 3. This is the optimum oscillation regime, where the wave amplitude at the output reaches the values of the clamped amplitude.²⁴ That is, in this regime beam electrons are trapped by the plasma wave around the coordinate $z=L$. In the optimal regime, the output amplitude increases significantly, and a steady-state oscillation regime is clearly established; the radiation efficiency is very high, of order 0.2.

As ξ is increased further, electron trapping occurs even for $z < L$; this causes the amplitude at the output to drop, which leads to a decrease in the radiation efficiency. Curves 5, 6, 7 illustrate this (points 5, 6, 7 on Fig. 1). It is also apparent that when ξ is larger than this optimal value, the output amplitude of the wave becomes chaotic.

At still higher values of ξ ($\xi=3.96$, point 8 on Fig. 1 and curve 8 in Fig. 2), the signal is observed to be highly chaotic, and the radiation efficiency drops abruptly.

Figure 3 shows the phase plane for the complex amplitude $a(\tau) = a_m(x=k_z L, \tau) \nu_0^{1/3}$: along the x axis we show $\text{Im}[\alpha(\tau)]$, while on the y axis we show $\text{Re}[\alpha(\tau)]$. Figure 3a corresponds to the pre-startup regime of oscillations (point 1 on Fig. 1). The uncoiled portion of the spiral corresponds to

excitation of waves by the front, while the central portion corresponds to attenuation of the signal after the front passes through. Figure 3b corresponds to the optimum regime (point 4 on Fig. 1). Figure 3c shows the onset of chaos (point 7 on Fig. 1). And, finally, Fig. 3d shows a strongly chaotic signal (point 8 on Fig. 1).

In all the cases we considered, we observed an abrupt increase in the oscillation amplitude at the output during the initial stage of the process. This increase lasts a time on the order of the beam transit time over the length of the system. This is because the rate at which the system begins to oscillate is initially characterized not by the gain $\text{Im}(\delta\omega)$, where $\delta\omega$ is determined from (20), but rather the usual spatial amplification of a forward wave excited by the beam front by stimulated Cerenkov emission. Soon after this, the backward wave begins to appear and the system becomes self-excited, i.e., acts as an oscillator (for values of ξ above startup).

Thus, the numerical simulation quantitatively confirms the conclusions of the linear theory regarding the existence of startup values of the structure parameters for which self-excitation of the plasma oscillator begins. Simulation of the nonlinear dynamics of these processes shows that optimum values of the parameters exist (which somewhat exceed startup) for which the steady-state value of the output signal is observed to reach its maximum level. Further increases in the beam current destroy the stationary oscillations, and chaotic oscillations are observed.

5. In conclusion, we will attempt to explain the high radiation efficiency. It is known that the wave amplitude reaches a maximum at the point where electrons are trapped by the beam.^{10,11,14,18} For small ξ , trapping does not occur for $z \leq L$, and the efficiency is low. For a certain optimum value of ξ , trapping takes place at $z=L$ and the efficiency is

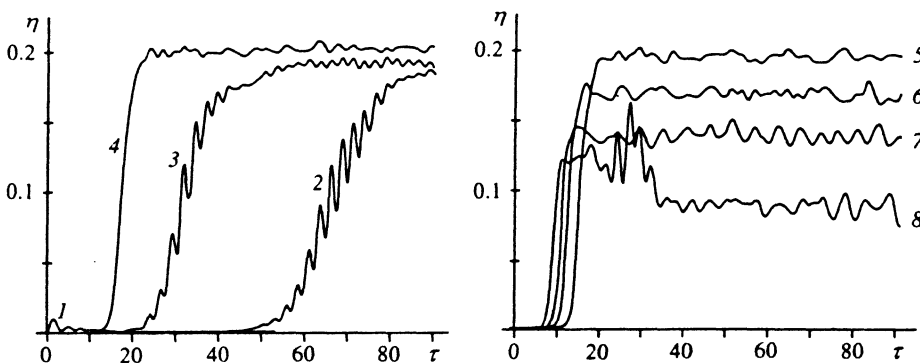


FIG. 2. Oscillation regimes: below-startup (1), slightly above startup (2,3), optimal (4), and strongly above startup (5-8).

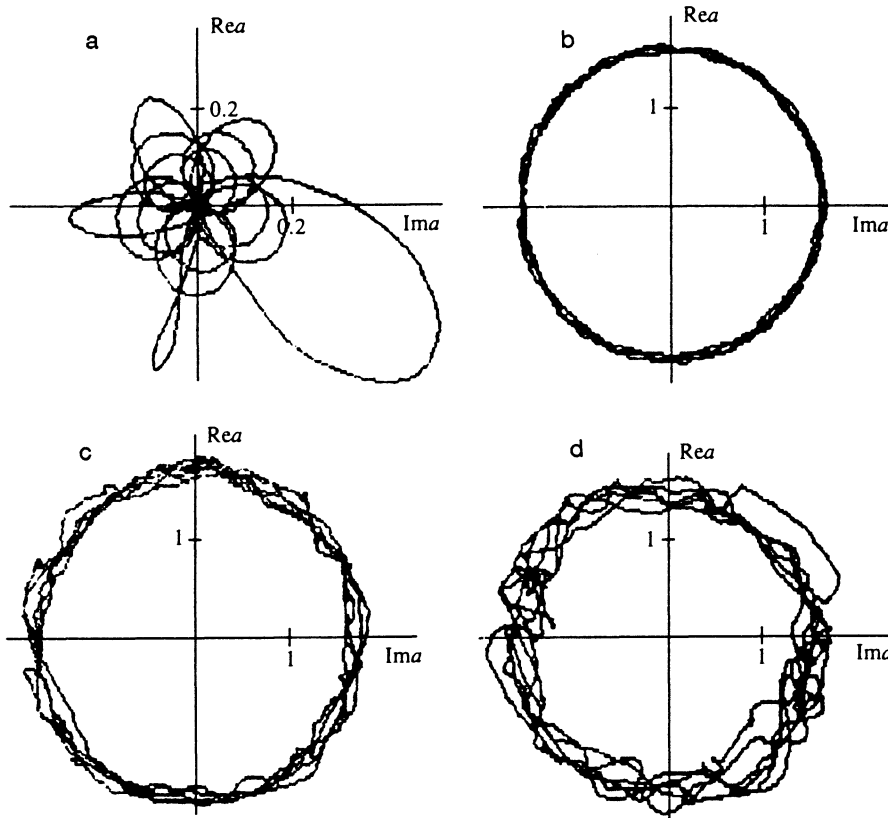


FIG. 3. Phase plane for the complex amplitude $\alpha(\tau)$: (a) below-startup oscillation regime (point 1 on Fig. 1); (b) optimal oscillation regime (point 4 on Fig. 1); (c) beginning of chaos (point 7 on Fig. 1); (d) fully developed chaotic oscillations (point 8 on Fig. 1).

a maximum. For larger ξ , trapping occurs for $z < L$ and the efficiency of radiation drops. Now, for comparatively small values of the current this would happen if we increased the value of ξ by increasing the length of the system L . However, things could be otherwise (and are for our calculations): for a fixed length, we can increase ξ by increasing ν_0 , i.e., the beam current. Nevertheless, it was shown in Refs. 10, 11, 25 that in general there is a certain current for which the Cerenkov instability mechanism changes to a nonradiating regime of negative-mass type.²⁶ In this case, the radiation efficiency drops abruptly due to a "phase transition." In our calculations, both factors were present, since our model includes everything that is necessary.

One more effect should be mentioned: the counterpropagating wave can be scattered by the beam with a frequency shift, causing a whole series of cascade processes to develop that probably have been observed experimentally.

¹Calculations for a beam with a smooth front lead to analogous results.

²The eigenfunctions φ_n correspond to the eigenvalue $k_{L,n}$.

³As a result of the Cerenkov instability, the beam density is modulated. If the beam current is large, this modulation is associated with a powerful longitudinal electric field at frequency $\omega < \omega_p$, [see (2)]. Since the dielectric permittivity of the plasma is negative at this frequency, the modulation of the beam will grow, causing further growth in the longitudinal field. In the literature, this process is referred to as an instability of negative-mass type.^{10,11,25}

¹M. V. Nezhlin, *Dynamics of Beams in Plasmas* (Energoizdat, Moscow, 1982) [in Russian].

²I. F. Kharchenko, Ya. B. Fainberg, R. M. Nikolaev *et al.*, *Zh. Éksp. Teor. Fiz.* **38**, 685 (1960) [Sov. Phys. JETP **11**, 493 (1960)].

³D. S. Bogdankevich, M. V. Kuzelez, and A. A. Rukhadze, *Usp. Fiz. Nauk* **133**, 3 (1981) [Sov. Phys. Usp. **24**, 1 (1981)].

⁴Ya. B. Fainberg, *Atomic Energy* **11**, 313 (1961) [in Russian].

⁵R. A. Demirkhanov, A. K. Gevorkov, A. F. Popov, and G. I. Zverev, *Zh. Tekh. Fiz.* **30**, 306 (1960) [Sov. Phys. Tech. Phys. **5**, 282 (1960)].

⁶M. V. Kuzelez, F. Kh. Mukhametzyanov, M. S. Rabinovich *et al.*, *Zh. Éksp. Teor. Fiz.* **83**, 1358 (1982) [Sov. Phys. JETP **56**, 780 (1982)].

⁷M. V. Kuzelez, V. R. Maikov, A. D. Poezd *et al.*, *Dok. Akad. Nauk SSSR* **300**, No. 5, 1112 (1988) [Sov. Phys. Dokl. **33**, 444 (1988)].

⁸P. S. Landa, *Self-Similarity in Distributed Systems* (Nauka, Moscow, 1983) [in Russian].

⁹V. N. Shevchik and D. I. Trubetskov, *Analytic Methods for Solving Problems in Microwave Electronics* (Sov. Radio, Moscow, 1970) [in Russian].

¹⁰M. V. Kuzelez and A. A. Rukhadze, *Electrodynamics of Dense Electron Beams in Plasma* (Nauka, Moscow, 1990) [in Russian].

¹¹N. I. Aizatskiĭ, *Fiz. Plazmy* **6**, 597 (1980) [Sov. J. Plasma Phys. **6**, 327 (1980)].

¹²L. S. Bogdankevich and A. A. Rukhadze, *Usp. Fiz. Nauk* **103**, 609 (1971) [Sov. Phys. Usp. **14**, 163 (1971)].

¹³A. F. Alexandrov, L. S. Bogdankevich, and A. A. Rukhadze, *Principles of Plasma Electrodynamics* (Springer-Verlag, New York (1984)).

¹⁴A. N. Kondratenko and V. M. Kuklin, *Principles of Plasma Electrodynamics* (Energoatomizdat, Moscow, 1978) [in Russian].

¹⁵M. V. Kuzelez and A. A. Rukhadze, *Zh. Tekh. Fiz.* **49**, 1182 (1979) [Sov. Phys. Tech. Phys. **24**, 654 (1979)].

¹⁶M. V. Kuzelez, V. A. Panin, A. P. Plotnikov, and A. A. Rukhadze, *Zh. Éksp. Teor. Fiz.* **101**, 460 (1992) [Sov. Phys. JETP **74**, 242 (1992)].

¹⁷A. A. Rukhadze, L. S. Bogdankevich, S. E. Rosinskiĭ, and V. G. Rukhlin, *Physics of High-Current Relativistic Electron Beams* (Atomizdat, Moscow, 1970) [in Russian].

¹⁸I. N. Onishchenko, A. R. Lipetskiĭ, N. G. Matsiborko *et al.*, *JETP Lett.* **12**, 281 (1970).

¹⁹B. Z. Katsenelenbaum, *High-Frequency Electrodynamics* (Nauka, Moscow, 1966) [in Russian].

²⁰Yu. L. Klimontovich, *Kinetic Theory of Nonideal Gases and Nonideal Plasmas* Pergamon, Oxford (1982).

²¹M. V. Kuzelez, V. A. Panin, A. A. Rukhadze, and D. S. Filipychev, *Pis'ma Zh. Tekh. Fiz.* **10**, 228 (1984) [Sov. Tech. Phys. Lett. **10**, 95 (1984)].

- ²²L. S. Bogdankevich, M. V. Kuzelev, and A. A. Rukhadze, *Fiz. Plazmy* **5**, 90 (1979) [*Sov. J. Plasma Phys.* **5**, 51 (1979)].
- ²³S. S. Kalmykova, *Zh. Éksp. Teor. Fiz.* **65**, 2250 (1973) [*Sov. Phys. JETP* **38**, 1124 (1973)].
- ²⁴R. I. Kovtun and A. A. Rukhadze, *Zh. Éksp. Teor. Fiz.* **58**, 1709 (1970) [*Sov. Phys. JETP* **31**, 915 (1970)].

- ²⁵M. V. Kuzelev and A. A. Rukhadze, *Usp. Fiz. Nauk* **152**, 285 (1987) [*Sov. Phys. Usp.* **30**, 507 (1987)].
- ²⁶V. V. Bogdanov, M. V. Kuzelev, and A. A. Rukhadze, *Fiz. Plazmy* **10**, 548 (1984) [*Sov. J. Plasma Phys.* **10**, 319 (1984)].

Translated by Frank J. Crowne